

## Cr/Pt Ohmic contacts to B<sub>12</sub>As<sub>2</sub>

S. H. Wang, E. M. Lysczek, Bangzhi Liu, and S. E. Mohney

*Department of Materials Science and Engineering and Materials Research Institute, The Pennsylvania State University, University Park, Pennsylvania 16802*

Z. Xu, R. Nagarajan, and J. H. Edgar

*Department of Chemical Engineering, Kansas State University, Manhattan, Kansas 66506-5102*

(Received 21 March 2005; accepted 8 June 2005; published online 20 July 2005)

Palladium, Pt, and Cr/Pt contacts to the wide band gap icosahedral boride semiconductor B<sub>12</sub>As<sub>2</sub> have been studied. All Pd and Pt contacts exhibited nonlinear *I-V* characteristics, while Cr/Pt contacts were Ohmic. The specific contact resistance was reduced from 6 Ω cm<sup>2</sup> as-deposited to 3 × 10<sup>-4</sup> Ω cm<sup>2</sup> after the Cr/Pt contacts were annealed at 750 °C for 30 s in Ar. Annealing at 600 °C or higher drastically reduced the semiconductor sheet resistance, whether annealing was performed before or after metallization. This apparent activation of the semiconductor is a likely cause for the improvement in the Ohmic contacts with annealing. © 2005 American Institute of Physics. [DOI: 10.1063/1.2001760]

There is great interest in increasing the energy density of power supplies to make systems incorporating microelectronics and microelectromechanical systems (MEMS) more mobile and autonomous. Chemical batteries have been the traditional source for mobile energy, but alternative sources such as fuel cells, flywheels, and photovoltaic devices are receiving increasing attention. Compact, lightweight, power sources are needed that can supply energy for years or even decades.<sup>1,2</sup> Radioisotope batteries are an attractive possibility, as their energy density could be as much as 10<sup>3</sup>–10<sup>4</sup> times higher by weight as chemical energy sources including batteries, microturbines, or fuel cells.<sup>2</sup>

Of the various possible nuclear to electrical conversion technologies, those employing the betavoltaic effect are the most direct. Beta cells produce electrical energy by coupling a radioactive beta emitter to a semiconductor junction<sup>3–6</sup> and are analogous to photovoltaics, with a beta source replacing light as the source of energy. Nearly 50 years ago, Rappaport *et al.*<sup>7</sup> demonstrated Ge and Si beta cells, but their power output rapidly decreased; in 14 h, the maximum power output decayed by half. Since this initial study, radiation damage to the semiconductor has remained the major impediment to the development of better beta cells.<sup>3,6</sup>

Recently, boron-based semiconductors have drawn attention for their unusual property of self-healing of radiation damage. In a study of electron irradiation effects on a series of boron compounds, Carrard *et al.*<sup>8</sup> demonstrated that neither defect clusters nor amorphization occurs in compounds containing boron icosahedra (twelve boron atom clusters). Regardless of the electron energy or flux employed (high enough to displace all boron atoms seven times), no defects were observed in the crystals by transmission electron microscopy (TEM). In addition to its radiation resistance, the boron-based semiconductor B<sub>12</sub>As<sub>2</sub> has a wide band gap (3.47 eV),<sup>9</sup> and theory predicts efficiencies greater than 20% are possible for wide band gap semiconductors.<sup>6</sup> These characteristics have prompted interest in B<sub>12</sub>As<sub>2</sub> for beta cells.<sup>10</sup>

The chemical vapor deposition of B<sub>12</sub>As<sub>2</sub> on 6H-SiC has recently been developed for the growth of high quality thin films.<sup>11–13</sup> The in-plane lattice constant for 6H-SiC is nearly one half that of B<sub>12</sub>As<sub>2</sub>, which facilitates epitaxial growth of

the films. There have been very few reports on the electrical properties of any of the icosahedral boride semiconductors ( $\alpha$ -rhombohedral boron, boron carbide, B<sub>12</sub>P<sub>2</sub>, or B<sub>12</sub>As<sub>2</sub>).<sup>14</sup> In general, only *p*-type conductivity has been observed for any of these compounds. Our preliminary results indicate that our B<sub>12</sub>As<sub>2</sub> films were all *p*-type as well.

To better establish the potential of B<sub>12</sub>As<sub>2</sub> for homojunction, heterojunction and Schottky barrier beta cells, investigations of the doping and device processing of B<sub>12</sub>As<sub>2</sub> are needed, including the development of a contact technology. In this study, Ohmic contacts to B<sub>12</sub>As<sub>2</sub> are reported. The effect of annealing on the resistance of B<sub>12</sub>As<sub>2</sub> epitaxial films is also described.

All contacts were fabricated on B<sub>12</sub>As<sub>2</sub> films deposited on Si-face, on-axis, semi-insulating 6H-SiC (0001) substrates. The deposition conditions were 1590 °C and 100 Torr for 40 min with 250 sccm of 2% AsH<sub>3</sub> in H<sub>2</sub>, 30 sccm of 1% B<sub>2</sub>H<sub>6</sub> in H<sub>2</sub>, and 5 slm of H<sub>2</sub> carrier gas. The nominal thickness of the B<sub>12</sub>As<sub>2</sub> film was 1.0 μm. Before metallization, samples were first degreased in acetone and methanol with ultrasonic agitation for 5 min each, rinsed with deionized (DI) water, and blown dry with N<sub>2</sub>. Where indicated, annealing of some samples prior to metallization was performed in ultrahigh purity (UHP) Ar in a rapid thermal annealing (RTA) furnace, followed by degreasing in acetone and methanol for 5 min each, and a rinse in DI water. The UHP Ar flowed through a Ti gettering furnace to remove O<sub>2</sub> prior to flowing through the RTA furnace. Photolithography was performed to fabricate patterns for specific contact resistance measurements. The circular transfer length method (CTLM) with contact diameter of 80 μm and gap spacings of 4, 8, 14, 20, 30, 50, and 75 μm was used.<sup>15</sup> At least four adjacent contacts were used for each CTLM calculation. Pre-metallization surface treatment was performed using buffered oxide etch (BOE) for 1 min, followed by rinsing the samples with DI water and blowing them dry with N<sub>2</sub>. Samples were then promptly loaded into a dc magnetron sputtering chamber, the chamber evacuated to a base pressure of 10<sup>-7</sup> Torr, and metal layers deposited. Liftoff of the metallization was performed in acetone with ultrasonic agitation followed by a methanol and DI water rinse before the

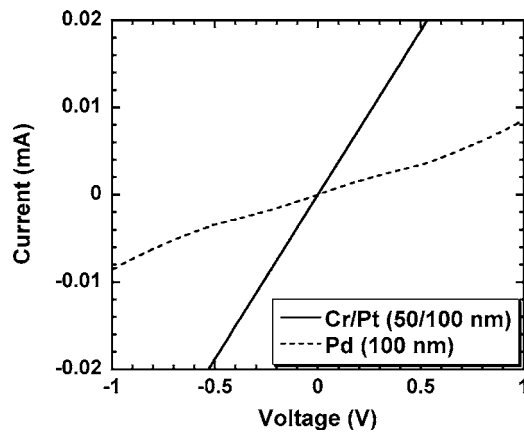


FIG. 1.  $I$ - $V$  characteristics of the Cr/Pt (50/100 nm) and Pd (100 nm) contacts annealed at 550 °C for 30 s in UHP Ar for a gap spacing of 4  $\mu\text{m}$ .

samples were blown dry. Cumulative annealing of the contacts was performed under UHP Ar in the RTA furnace for 30 s each from 260 °C to 750 °C.

Cr/Pt (50/100 nm), Pd (100 nm), and Pt (150 nm) contact samples were compared. Palladium and Pt contacts were chosen because they have high work functions, while Cr/Pt contacts were chosen because there are conductive chromium borides with excellent thermal stability. For the Cr/Pt contacts, Cr was deposited directly on the  $\text{B}_{12}\text{As}_2$ , followed by deposition of the Pt. Figure 1 shows the  $I$ - $V$  characteristics of the Cr/Pt and Pd contacts annealed at 550 °C for 30 s in UHP Ar for a gap spacing of 4  $\mu\text{m}$ . Linear  $I$ - $V$  curves were observed for all three Cr/Pt (50/100 nm) contact samples, whereas the two Pd (100 nm) and one Pt (150 nm) samples exhibited nonlinear  $I$ - $V$  characteristics before and after annealing. Similar results for Cr/Pt and Pt contacts were also obtained on other  $\text{B}_{12}\text{As}_2$  epilayers. The specific contact resistance and semiconductor sheet resistance for the Cr/Pt (50/100 nm) contacts are plotted as a function of annealing temperature in Figs. 2 and 3, respectively. A high specific contact resistance of 6  $\Omega\text{cm}^2$  and semiconductor sheet resistance of  $1 \times 10^8 \Omega/\square$  were observed for the as-deposited condition, corresponding to a resistivity of  $1 \times 10^4 \Omega\text{cm}$ . These values were significantly decreased after annealing at 600 °C or higher. After the Cr/Pt contacts were

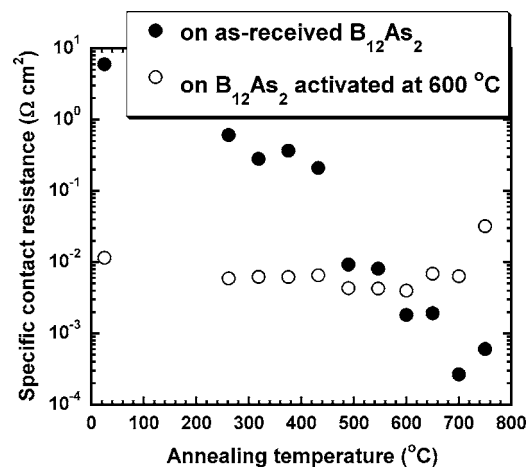


FIG. 2. The specific contact resistance of the Cr/Pt (50/100 nm) contacts to (●) as-received  $\text{B}_{12}\text{As}_2$  and (○)  $\text{B}_{12}\text{As}_2$  activated at 600 °C for 30 s in UHP Ar.

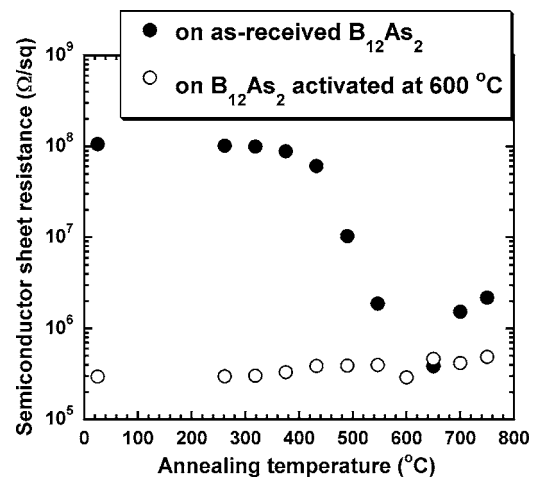


FIG. 3. The semiconductor sheet resistance of the Cr/Pt (50/100 nm) contacts to (●) as-received  $\text{B}_{12}\text{As}_2$  and (○)  $\text{B}_{12}\text{As}_2$  activated at 600 °C for 30 s in UHP Ar.

annealed at 700 °C for 30 s in UHP Ar, their specific contact resistance and the semiconductor sheet resistance dropped to  $3 \times 10^{-4} \Omega\text{cm}^2$  and  $2 \times 10^6 \Omega/\square$ , respectively. Consistent with our observations for the Cr/Pt contacts, the resistance of the Pd contacts was reduced after annealing at 600 °C, but the  $I$ - $V$  curves were still nonlinear. Moreover, the Pd contact's surface morphology degraded annealing at 600 °C for 30 s in Ar. An agglomeration or dewetting of the Pd film is shown in Fig. 4. The Pt contacts also showed visible degradation in surface morphology after annealing at 550 °C, and the contacts never became Ohmic. In contrast, the surface morphology of the Cr/Pt contacts remained smooth after annealing at 600 °C for 30 s in UHP Ar, as shown in Fig. 5. The lower specific contact resistance and greater thermal stability of the Cr/Pt contacts indicate that they are better than Pd and Pt for making Ohmic contact to  $\text{B}_{12}\text{As}_2$ .

As shown in Figs. 2 and 3, annealing greatly reduced the specific contact resistance of the Cr/Pt contacts and the semiconductor sheet resistance, which indicates that the heat treatment affects not just the contact but also the semiconductor. Auger depth profiling was performed to examine the effect of annealing the Cr/Pt contacts and the semiconductor prior to metallization (not shown). There was no evidence for reaction of  $\text{B}_{12}\text{As}_2$  with the SiC substrate or any compositional shift of the  $\text{B}_{12}\text{As}_2$  semiconductor (within 1 at %). To further investigate the effect of the heat treatment, additional samples were annealed at 550, 600, and 750 °C for 30 s in

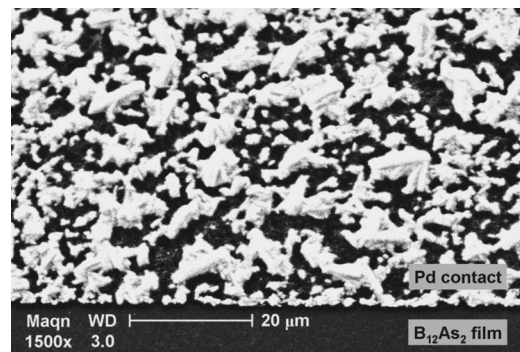


FIG. 4. SEM image of the Pd (100 nm) contact after annealing at 600 °C for 30 s in UHP Ar. The edge of the patterned contact is shown at the bottom of the image.

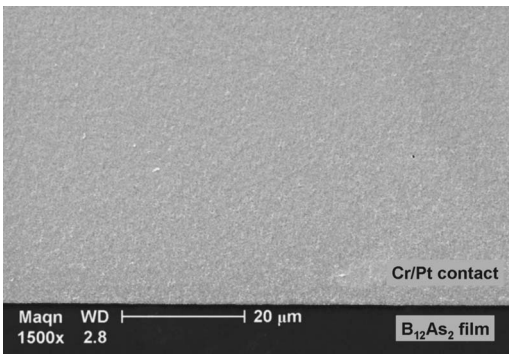


FIG. 5. SEM image of the Cr/Pt (50/100 nm) contact after annealing at 600 °C for 30 s in UHP Ar. The edge of the patterned contact is shown at the bottom of the image.

UHP Ar prior to metallization (referred to hereafter as activation annealing). Cr/Pt contacts were next deposited on the activated semiconductor film, and  $I$ - $V$  characteristics were measured on the contacts for the as-deposited condition and after annealing for 30 s in UHP Ar from 260 °C to 750 °C.

Figure 2 shows the specific contact resistance of the Cr/Pt contacts versus annealing temperature for the epilayers activated at 600 °C for 30 s in UHP Ar. The corresponding semiconductor sheet resistance is shown in Fig. 3. Similar results were obtained for Cr/Pt contacts on  $B_{12}As_2$  epilayers activated at 550 °C and 750 °C. As shown in Fig. 2, the specific contact resistance decreased only slightly from  $1 \times 10^{-2} \Omega \text{ cm}^2$  for the as-deposited condition to  $4 \times 10^{-3} \Omega \text{ cm}^2$  when contacts to the semiconductor activated at 600 °C were later annealed at 600 °C. Furthermore, the semiconductor sheet resistances remained in the range of  $10^5$ – $10^6 \Omega/\square$  with annealing of the contacts. Further annealing of the contacts at 750 °C increased the specific contact resistance.

The specific contact resistance and semiconductor sheet resistance are significantly lower before annealing the metallization when contacts are prepared on the activated samples (Figs. 2 and 3). Annealing of the contacts to these layers changed these values only slightly. Thus, the semiconductor sheet resistance appears to have approached a minimum value during the activation anneals. Although the mechanism

by which annealing reduces the semiconductor sheet resistance is not currently known, it is conceivable that hydrogen incorporated during growth of the semiconductor is released or redistributed during annealing, as occurs in Mg-doped GaN. If such a change results in an increase in the concentration of electrically active acceptors, the resistivity of the semiconductor and the specific contact resistance would both be reduced.

In summary, Pd and Pt contacts to  $B_{12}As_2$  exhibited non-linear  $I$ - $V$  characteristics, whereas Ohmic contacts were achieved using Cr/Pt contacts. Annealing the  $B_{12}As_2$  epilayers decreased the specific contact resistance of the Cr/Pt contacts and the semiconductor sheet resistance, whether performed before or after the metal contacts were deposited. The activation anneals prior to metallization reduce the specific contact resistance and the semiconductor sheet resistance, which might be attributed to an increase in acceptor concentration in the  $B_{12}As_2$  epilayers after annealing.

<sup>1</sup>K. E. Bower, Yu. A. Baranel, Yu. G. Shreter and G. W. Bohnert, *Polymers, Phosphors, and Voltaics for Radioisotope Microbatteries*, 1st ed. (CRC Press, Boca Raton, FL, 2002).

<sup>2</sup>K. E. Bower, A. F. Rutkiewicz, C. C. Bower, and S. M. Yousaf, in Ref. 1, pp. 441–457.

<sup>3</sup>A. G. Kavetsky, S. P. Meleshkov, and M. M. Sychov, in Ref. 1, pp. 1–38.

<sup>4</sup>M. M. El-Wakil, *Nuclear Energy Conversion*, 1st ed. (Intext Educational, Scranton, PA, 1971), Chap. 15, pp. 500–517.

<sup>5</sup>W. R. Corliss, *Radioisotopic Power Generation* (Prentice-Hall, Englewood Cliffs, 1964).

<sup>6</sup>L. C. Olsen, 9th Intersociety Energy Conversion Engineering Conference Proceedings, San Francisco, 1974 (ASME, New York, 1974), pp. 754–762.

<sup>7</sup>P. Rappaport, J. J. Loferski and E. G. Linder, *RCA Rev.* **17**, 100 (1956).

<sup>8</sup>M. Carrard, D. Emin, and L. Zuppiroli, *Phys. Rev. B* **51**, 270 (1995).

<sup>9</sup>G. A. Slack, T. F. McNelly, and E. A. Taft, *J. Phys. Chem.* **44**, 1009 (1983).

<sup>10</sup>T. L. Aselage and D. Emin, U.S. Patent No. 6 479 919 (2001).

<sup>11</sup>R. H. Wang, D. Zubia, T. O'Neil, D. Emin, T. Aselage, W. Zhang, and S. D. Hersee, *J. Electron. Mater.* **29**, 1304 (2000).

<sup>12</sup>W. M. Vetter, R. Nagarajan, J. H. Edgar, and M. Dudley, *Mater. Lett.* **58**, 1331 (2004).

<sup>13</sup>R. Nagarajan, Z. Xu, J. H. Edgar, F. Baig, J. Chaudhuri, Z. Rek, E. A. Payzant, H. M. Meyer, J. Pomeroy, and M. Kuball, *J. Cryst. Growth* **273**, 431 (2005).

<sup>14</sup>O. A. Golikova, *Phys. Status Solidi A* **51**, 11 (1979).

<sup>15</sup>G. S. Marlow and M. B. Das, *Solid-State Electron.* **25**, 91 (1982).